$$\frac{G}{RT} = \frac{n_0\mu_0}{RT} + \sum_{j\neq 0} n_j \left[\ln m_j\lambda_j^{\theta} - 1\right] + \text{D.H.}$$

$$+ \sum_{i\neq 0}\sum_{j\neq 0} n_i m_j \left[M_0 A_{ij} - \frac{1}{2} M_0\right] \quad \text{(B6)}$$

The Debye-Hückel term can now be used in its familiar form. Thus

$$\text{D.H.} = -\frac{2}{3}\alpha\sqrt{I}\,\tau(\mathbf{B}a\sqrt{I}) \sum_j z_j^2 n_j \quad \text{(B7)}$$

where

$$\tau(\delta) = \frac{3}{\delta^3}\left[\ln(1+\delta) - \delta + \frac{1}{2}\delta^2\right]$$

Taking the partial derivative with respect to the number of moles species i, we obtain the activity coefficient

$$\ln\gamma_i = \frac{\partial(G/RT)}{\partial n_i} - \ln m_i\lambda_i^{\theta} \quad \text{(B8)}$$

$$= \frac{-\alpha z_i^2\sqrt{I}}{1+\mathbf{B}a\sqrt{I}} + 2\sum_{j\neq 0}\beta_{ij} m_j$$

where $\beta_{ij} = M_0(A_{ij} - 0.5)$.

For all practical purposes the product $\mathbf{B}a$ is unity when I is expressed in units of molality.

Manuscript received September 11, 1974; revision received November 12 and accepted November 13, 1974.

Wall Mass Transfer in Laminar Pulsatile Flow in a Tube

Wall mass transfer was measured in fully developed pulsating laminar flow in a tube using the diffusion-controlled electrode technique. The average Reynolds number, pulsating frequency and amplitude, and length of the mass transfer surface were the independent variables studied. The results are given in the form of the amplitude ratio and phase angle of the pulsating wall transfer rate. At lower frequencies the amplitude and phase were found to be correlated by the variable $\omega_d^2\, Gz^{-2/3}$ in accordance with theory. At higher frequencies an empirical correlation with the variable $\omega_d^2\, Gz^{-1/3}(L/D)^{1/3}$ was found. While this may show some deficiency in the usual theoretical model, it is also possible that other causes such as nondevelopment of the flow are responsible. Time-averaged transfer rates were found to be only slightly different from the corresponding steady flow transfer rates in the range of variables investigated.

RUTTON D. PATEL
JOHN J. MCFEELEY

Department of Chemical Engineering
Polytechnic Institute of New York
Brooklyn, New York 11201

and
KENNETH R. JOLLS

Department of Chemical Engineering
Iowa State University
Ames, Iowa 50010

SCOPE

Mass or heat transfer in pulsatile flow is of importance in many areas. Examples are pulsed operation of extraction columns and heat exchangers, transport in the cardiovascular system, etc. When the velocity of a fluid flowing past a surface transferring mass has superimposed on it a time-varying component, then the mass transfer rate is also found to vary with time around some mean value. This mean or time averaged value is often, but not always, found to be greater than that for the corresponding steady flow. Such effects are of obvious interest since they offer the possibility of improving the performance of process equipment. Another question of interest is the relation between the fluctuating transfer rate (or equivalently, the mass transfer coefficient) and the fluctuating velocity. More specifically, we wish to know how rapidly the transfer rate varies upon the inception of a velocity perturbation, and how the magnitude of the fluctuation in mass transfer rate depends on the magnitude of the velocity fluctuation. These questions are answered if the phase difference and the amplitude ratio of the fluctuating transfer rate to the fluctuating velocity field are known.

There has been extensive work in this area, both theoretical and experimental, dealing with questions such as local fluctuating transfer rates, time-averaged transfer rates, etc. in various geometries, such as pulsed extraction columns, flow in tubes, flow past plates, etc. Conflicting results have been reported. Some authors find the time-

Correspondence concerning this paper should be addressed to R. D. Patel. J. J. McFeeley is with Polaroid Corporation, Cambridge, Massachusetts.

averaged transfer rates to be higher than those for steady flow, others find them to be lower.

In this work a simple first-order theoretical model was developed and an experimental study was conducted of wall mass transfer in a tube in which a fluid was flowing in pulsatile laminar flow. Wall transfer rates were measured using the diffusion-controlled electrode method, which has the advantage that the wall is not eroded and that the mass transfer coefficient may be directly related to the current from the electrode. A Fourier analysis was made of the fluctuating transfer rate. The amplitude ratio and the phase angle of the first harmonic of the fluctuating mass transfer coefficient to the fluctuating velocity were found for various amplitudes and frequencies of pulsation, various Reynolds numbers, and different lengths of the mass transfer surface.

CONCLUSIONS AND SIGNIFICANCE

The theoretical model suggests that the amplitude ratio and phase angle of the fluctuating transfer coefficient are related to a single dimensionless correlation variable $X_1 = \omega_d^2\ Gz^{-2/3}$. This is consistent with a similar local variable developed by Pedley (1972).

Most of the experimental data fell in the range of high dimensionless frequencies according to the results of Alabastro and Hellums (1969). Data for the amplitude ratio were more accurate than the phase data because of the experimental techniques used. In general, the trend of the data was as expected. The amplitude ratio of the first harmonic of the fluctuating transfer coefficient was found to decrease with increasing frequency and increasing length of the transfer surface. The phase lag under these conditions was found to increase. The effect of Reynolds number was small.

At lower values of X_1 the data for amplitude and phase correlated fairly well with X_1 although the phase data showed much poorer agreement. In accordance with theory, no effect was observed of Reynolds number or mass transfer length. In this lower frequency range the function A, which is related to amplitude [see Equation (14)], reached an asymptotic value of $A = 0.825$.

At higher frequencies (larger X_1) the data plotted as A versus X_1 yielded different curves for various Reynolds numbers and frequencies. An empirical correlation variable $X_2 = \omega_d^2\ Gz^{-1/3}(L/D)^{1/3}$ was found to correlate the data for A in a single curve with fair agreement. An empirical curve fit of A against X_2 was obtained—Equation (18). The phase data for higher frequencies, plotted as φ [Equation (15)] were found to be in general agreement with the theoretical curve calculated using the empirical constants of Equation (18). There was considerable scatter, however.

It cannot be said with certainty that the theoretical prediction is incorrect for large values of X_1, although the present data seem to indicate this. It is possible that the flow near the transfer surface was not the fully developed flow assumed so that the conditions underlying the theory were not fulfilled. Only further experiments can establish this. On the other hand, the theoretical development neglects diffusion in the flow direction, and at least for some of the data, this may be the cause for the discrepancy.

Rather small changes were found in the time averaged mass transfer rates over the corresponding rates for steady flow. This is in accordance with Alabastro and Hellums (1969) because, in the range of variables investigated, the second harmonic of the fluctuating coefficient was found to be very small.

It appears that the present work reports the first experimental measurements of amplitude and phase of the fluctuating mass transfer coefficient in pulsatile flow. Most previous data were for the time-averaged coefficients only.

Mass transfer in pulsatile flow is important in many areas of science and engineering. Applications include pulsed operation of extraction columns, studies of turbulence near a wall by diffusion-controlled electrodes, transport of species between the arterial wall and flowing blood, etc. Recently several theoretical studies of this problem have appeared. The experimental results of previous workers have not been entirely consistent and much work needs to be done in this area.

The fluid mechanical problem of pulsatile flow in tubes has been studied extensively because of its application to arterial blood flow. McDonald (1960) has given a review of this area. Other important studies have been made by Womersley (1955) and Atabek and Chang (1961) on the flow field in a rigid tube. In this work we are primarily interested in wall heat or mass transport in such a flow field. Richardson (1967) has reviewed prior work in this area in his review of the effect of sound and vibrations on heat transfer. Below are cited some of the more pertinent works.

The earliest measurements seem to be those of Martinelli et al. (1943) who studied heat transfer at low pulsing frequencies in a vertical tube. Haveman and Rao (1954) have shown that the average Nusselt number decreases with frequency up to a critical value and then increases with a further increase in frequency. Ostrach (1952) and also West and Taylor (1952) have studied the effect of heat transfer in the laminar flow of a fluid with pulsations superimposed upon a steady flow. Similar studies by Baird et al. (1966), Mueller (1957), Sozin (1965), and Shirotsuka (1957) have been done on the turbulent flow of an incompressible fluid.

Krusak and Smith (1963) observed the dissolution of β-naphthol from the wall of an absorption column and have shown that a definite increase in the mass transfer rate results during pulsed flow. The increase is most pronounced at low average flow rates as has been confirmed by other workers. On the other hand, Mueller (1957) has found the average Nusselt number to be less than the corresponding steady flow Nusselt number for turbulent flow.

Theoretical approaches to the problem have been made by Lighthill (1954), Alabastro and Hellums (1969), and Pedley (1972). Lighthill used a perturbation method (to first order only) to study the effects of small fluctuations in the free stream velocity on the momentum and thermal boundary layers on an immersed body. He found no change in the time-averaged heat transfer rate at the wall.

Alabastro and Hellums (1969) have made a theoretical study of wall mass transfer in pulsating laminar flow in a tube. They have shown that by making a perturbation expansion to second order it is possible to predict the change in time-averaged mass transfer rate at the wall. They present their results in the form of amplitude and phase angle of the first two harmonics of the wall transfer rate as a function of frequency. Unfortunately the bulk of their results are for the local transfer rate (that is, its point value) at a particular dimensionless distance from the leading edge of the mass transfer surface. It is difficult to compare their predictions with experimental data because only the area averaged transfer rate can be conveniently measured. An important contribution has been made by Ling (1963) who established the limits of the length of the transfer surface on the validity of a boundary layer solution to the problem. Ling's range of validity appears to be different from that given by Alabastro and Hellums. Pedley (1972) has considered wall heat transfer in a velocity field characterized by a known periodic wall velocity gradient. Numerical results are given for the instantaneous wall transfer rate.

In this paper results are presented of an experimental study of wall mass transfer in fully-developed pulsating laminar flow in a tube. Wall transfer rates were measured using the diffusion-controlled electrode technique which has the advantage that the wall surface is not abraded or distorted during the experiment, and also that the transfer rate is readily measured as the current in the external circuit.

THEORY

Womersley (1955) has obtained the velocity profile for the case of fully-developed laminar flow in a rigid tube under the action of a periodic pressure gradient of the form

$$-\frac{\partial p}{\partial x} = p_s(1 + \lambda_p e^{i\beta t}) \tag{1}$$

For the problem at hand the velocity near the wall is of interest. Since the Schmidt number for liquids is large (of order 10^3), the concentration boundary layer is very thin so that a linear velocity distribution may be assumed. The slope of this distribution at the wall is taken from the exact solution of Womersley so that the linearized profile assumed here is given by

$$u(y, t) = \frac{U_0 y}{R}\{4 + \lambda_p \gamma e^{i\beta t}\} \tag{2}$$

where

$$\gamma = -\frac{8i^{1/2}}{\omega_v}\frac{J_1(\omega_v i^{3/2})}{J_0(\omega_v i^{3/2})} \tag{3}$$

and

$$\omega_v = \left(\frac{\beta R^2}{\nu}\right)^{1/2} \tag{4}$$

is a dimensionless frequency parameter often called the Womersley number.

We now consider the problem of diffusion of species to or from an element situated at the wall surface in the above flow field. The x-coordinate is in the flow direction and the y-coordinate is normal to it. The boundary layer equation for the dimensionless concentration c is

$$\frac{\partial c}{\partial t} + u\frac{\partial c}{\partial x} = \mathcal{D}\frac{\partial^2 c}{\partial y^2} \tag{5}$$

with boundary conditions

$$\begin{aligned} c\,(x, y = 0, t) &= 0 \\ c\,(x, y = \infty, t) &= 1 \\ c\,(x = 0, y, t) &= 1 \end{aligned} \tag{6}$$

It should be noted that diffusion in the flow direction has been neglected in comparison to the convection term. In usual boundary layer theory this is valid except near the leading edge. Ling (1963) has shown that this assumption is valid and the boundary layer solution is accurate for all values of x if

$$Pe > 5000 \tag{7a}$$

Pedley (1972), using Ling's results, has observed that the boundary layer solution gives transfer rates accurate to 5% even for smaller Peclet numbers in the region

$$0.5\,Pe^{-1/2} < x/L < 1 - 0.7\,Pe^{-1/2} \tag{7b}$$

where $Pe = 4U_0L^2/R\mathcal{D}$ is the Peclet number based on the length of the mass transfer surface. Alabastro and Hellums (1969) have presented such a boundary layer analysis, but give a range of validity different from the above. It appears that they have not considered the errors inherent in neglecting streamwise diffusion near the leading and trailing edges. Pedley (1972) also gives a boundary layer solution using matched asymptotic expansions but gives numerical results only for the case where γ is constant. [Pedley assumed a known periodic wall velocity gradient rather than a periodic pressure gradient as in Equation (1).] The analysis below follows the work of Alabastro and Hellums quite closely but arrives at solutions involving a single parameter rather than the two parameters ω and ξ used by Alabastro. Since the analysis is very similar to that of Alabastro, only a brief outline is given. Details may be found in McFeeley (1972).

A perturbation solution to Equation (5) is sought in the form

$$c(x, y, t) = c_0(x, y) + \lambda_p c_1(x, y, t) + 0(\lambda^2) \tag{8}$$

It should be noted that the perturbation expansion is truncated after the linear term in contrast to Alabastro. It will be apparent below that the data obtained show that succeeding terms are of much smaller order than c_1. The quantity of interest is the mass transfer coefficient at the wall given by

$$K = \mathcal{D}\left.\frac{\partial c}{\partial y}\right|_{y=0}$$

and more importantly the spatially-averaged coefficient over the length of the transfer surface

$$\langle K\rangle = \frac{1}{L}\int_0^L K\,dx$$

since this is the quantity that is measured. It may be shown that $\langle K\rangle$ can be expressed as the sum of a steady and a fluctuating term as

$$\langle K\rangle = \langle K_s\rangle\{1 + \lambda_c e^{i\beta t}\}$$

where

$$\lambda_c = \frac{\langle K_f\rangle}{\langle K_s\rangle}\lambda_p \tag{9}$$

is complex and is an amplitude ratio of the fluctuating coefficient. Subscripts s and f denote steady and fluctuating, respectively. The term $\langle K_s\rangle$ is related to c_0 which is just the Leveque solution and is given by Alabastro. The solution for the fluctuating part is obtained following the procedure of Alabastro for the first order term c_1.

The low frequency solution yields

$$\lambda_c = \lambda_p \frac{\gamma}{12} (1 + i\, 2^{1/3}\, a\, \omega_d^2\, Gz^{-2/3}) \qquad (10)$$

where

$$\omega_d = \omega_v\, Sc^{1/2} \qquad (11)$$

and a is a constant. Thus the variable $\omega_d^2 Gz^{2/3}$ determines the solution. This variable is identical to the form of the variable ϵ used by Pedley (1972) and the variable ξ in a recent theoretical work by McMichael and Hellums (1974). The constant a is obtained by a comparison of Equation (10) with solutions given by Reiss (1962) and Mitchell (1965) yielding

$$a = -\,0.25285\ (3/2)^{1/3}\ \Gamma\ (1/3)$$

The low frequency solution for the mass transfer ratio R_{cp} thus becomes

$$R_{cp} = \frac{\langle K_f \rangle}{\langle K_s \rangle} = \frac{\lambda_c}{\lambda_p} = \frac{\gamma}{12} (1 - 0.97739\, \omega_d^2 Gz^{-2/3}\, i) \qquad (12)$$

A high frequency solution for the fluctuating part may be obtained in the form

$$R_{cp} = \frac{\langle K_f \rangle}{\langle K_s \rangle} = \frac{\lambda_c}{\lambda_p} = \frac{\gamma}{12} \frac{1}{1 + 0.97739\, \omega_d^2 Gz^{-2/3}\, i} \qquad (13)$$

The modulus of R_{cp} referred to as A_{cp} and the phase angle Φ_{cp} can be calculated from Equations (12) and (13) and compared with the experimental data. As will be detailed below, most of the experimental data fell in the intermediate to high frequency range. Even in the high frequency range the correlation with the variable $\omega_d^2\, Gz^{-2/3}$ was not very good. Better agreement was obtained using the variable $\omega_d^2\, Gz^{-1/3}(L/D)^{1/3}$. This indicates a different dependence on the Reynolds and Schmidt numbers and suggests that the conventional analysis neglecting diffusion in the flow direction needs re-examination.

Finally it should be mentioned that the truncation of Equation (8) to the first-order term precludes any calculation of time-averaged mass transfer enhancement. As pointed out by Alabastro and Hellums (1969) the second-order term must be included to predict enhancement of the time averaged mass transfer rate.

EXPERIMENTAL TECHNIQUE

The experimental equipment was designed to produce, within a horizontal tube, a fully-developed laminar flow with a small sinusoidal perturbation superimposed on a steady velocity. Wall mass transfer rates were measured using the well known diffusion-controlled electrode technique [for example, Eisenberg et al. (1954), van Shaw et al. (1963), etc.]. Only a brief description of the equipment is given here; details are given by McFeeley (1972).

The flow loop is shown in Figure 1. The electrolyte flowed by gravity from the constant head tank to the variable head tank. The time-averaged liquid flow from the variable head tank was regulated by the flow control valve FC-1. From this valve, the solution passed through a fine mesh nylon filter and into the variable head tank. The average height of the liquid in this variable head tank was controlled by the flow control valve FC-2 situated at the outlet of the tank.

The solution flowed from the variable head tank through a 2.5-cm O.D. nickel anode, the upstream anode, into the control valve and finally through a flow straightener consisting of a bundle of 26 Teflon tubes (14 AWG, thin walled). At this point a nearly plug, laminar, velocity profile is produced. This is the beginning of the hydrodynamic entry region and conforms to the entrance boundary condition specified in the solution of Atabek and Chang (1961). The solution flowed from

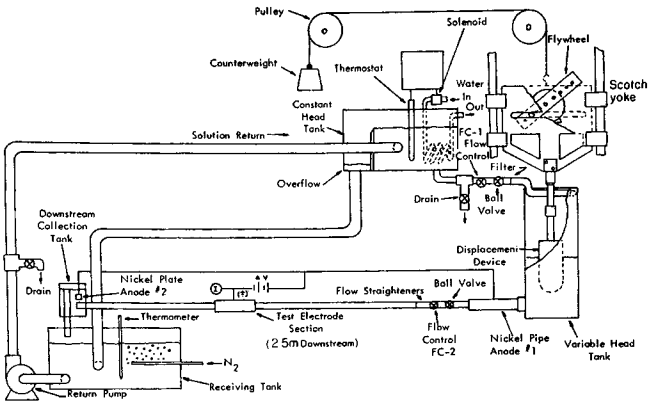

Fig. 1. Flow loop.

the flow straightener into a rigidly clamped, horizontal PVC pipe 1.427-cm internal diameter. The distance from the flow straightener to the test section cathodes was 2.5 m., corresponding to 175 pipe diameters. This entrance length is some three times greater than the maximum entrance length for steady flow. It is estimated that this length is also sufficient for fully-developed flow in the pulsatile case although it is difficult to check this from the results of Atabek and Chang (1961). After traversing the test section the solution flowed into a small collection tank 1.22 m beyond the test section. The collection tank was designed with an overflow pipe to maintain a liquid-full test line free of bends or other flow disturbances. The downstream anode, a 7.6 cm square sheet of nickel, 0.051 cm thick, was placed in this collection tank. The use of two anodes ensures the isolation of the test electrode from any external current sinks (for example, the stainless steel casing of the pump).

The solution overflowed from this collection tank into the receiving tank, which also received the overflow from the constant head tank. Since dissolved oxygen interferes with the ferricyanide polarization plateau, nitrogen was added through a nitrogen sparger. The variable head tank was covered with a plastic sheet and the solution maintained under a nitrogen blanket. All tanks were constructed from annealed lucite and were painted to avoid exposing the ferricyanide to light which would cause irreversible decomposition. The solution temperature was maintained at 24.8°C by a thermostat situated in the constant head tank.

Pulsations in the height of the liquid level produced the variable flow field in the horizontal pipe. This pure sinusoidal variation in the height was produced by a displacement device immersed in the liquid and situated at the end of a counterbalanced scotch yoke mechanism. This scotch yoke transformed the rotational motion of the flywheel into the vertical, sinusoidal, motion of the displacement device. The flywheel was driven by a 1/15 HP gear-reduced motor controlled by a variable speed SCR (Bodine Electric Co., Type ASH401) capable of controlling the motor speed to within 1% in the range of 0.42 to 22 rev./min. The magnitude of the height fluctuation was governed by the stroke of the connecting pin on the flywheel. The maximum penetration of the displacement device into the constant head tank was controlled by the length of the rod connecting the scotch yoke and the displacement device. The displacement device consisted of a machined lucite cylinder whose diameter determined the change in height of the liquid in the tank. Thus by changing the motor speed, the stroke of the flywheel pin, and the diameter of the displacement device and its depth of penetration, the amplitude and frequency of the fluid depth in the tank could be varied over a wide range. The time-averaged depth of the fluid was controlled by valve FC-2. At low amplitudes and frequencies the equipment produced a sinusoidal pressure gradient superimposed on a steady value in the pipe.

The test section (Figure 2) consisted of nine parallel annular plates of nickel, serving as electrodes, each of a different size, spaced by 0.635-cm thick rings of polystyrene. Lucite was not used here due to its tendency to swell after prolonged contact with water. Each electrode was cut from flat stock and precisely machined to eliminate any burrs. A 5-cm diameter

ELECTRODE LENGTHS

1) 0.2108 cm.
2) 0.6350 cm.
3) 0.4064 cm.
4) 0.2007 cm.
5) 0.0991 cm.
6) 0.0635 cm.
7) 0.0254 cm.
8) 0.0127 cm.
9) 0.2032 cm.

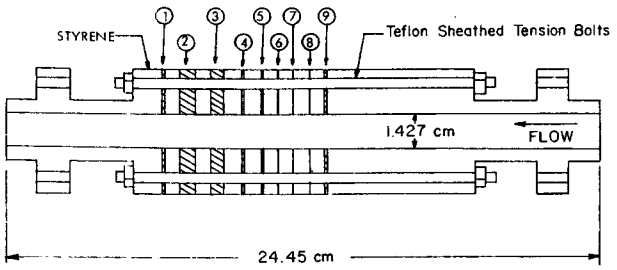

Fig. 2. Test section.

bar of styrene was reamed and then polished to the exact ID of the PVC pipe. Each styrene section was then cut from this bar and stacked alternately with nickel on a mandrel made from drill rod. The insulated tension bolts were then inserted and fastened and the entire assembly was carefully removed from the mandrel. This procedure was used instead of simultaneously machining the styrene and nickel together since they differ greatly in hardness.

A specially constructed profilometer used to measure the inside smoothness of the test section showed the average roughness to be about 5×10^{-4} cm. The electrodes were electrolytically cleaned from time to time to eliminate poisoning. Of the nine electrodes available, three were virtually of the same length and served as checks against one another. The largest (number 2) was not used because its current level was too high for the test equipment.

The electrolyte used consisted of an equi-molar solution of potassium ferricyanide-potassium ferrocyanide of about 0.01 M contained in a 2N solution of sodium hydroxide as a supporting electrolyte. A potential difference (in the diffusion controlled region) was imposed between the particular cathode under test and the two anodes. The current produced in the external circuit is directly proportional to the mass flux at the cathode surface, and, since in the diffusion controlled region the wall concentration is zero, the mass transfer coefficient. The output of the test electrode was an unsteady current with an average value in the range of 0.1 to 1.0 ma. Superimposed on this average value was a periodic fluctuation of amplitude about 0 to 5% of the average value. The cathode current was measured using a Heath EUA 19-2 polarographic module (D. C. Heath & Co.) together with Heath EUA 19-B operational amplifiers. A high accuracy was necessary to detect the small periodic fluctuations. Therefore, instead of recording the output from the polarography module, a digital technique using a digital voltmeter and a timing module connected to an analog computer was used to measure the signal.

The phase lag of the current with respect to the oscillations of the displacement device was also measured. Tests run on known periodic signals showed that the first harmonic could be measured with less than 0.5% error using this technique. Details are given by McFeeley (1972) and will appear in a forthcoming publication.

The digital current data were fitted to a Fourier series to obtain the steady current, and the amplitudes and phases of the first three harmonics. In general, the amplitude of the first harmonic was found to be one or two orders of magnitude greater than the amplitude of the second harmonic, implying that the current fluctuations were almost purely sinusoidal in the range of variables investigated. The third harmonic was even smaller. The small magnitudes of the higher harmonics made it difficult to interpret the results because of large relative errors so that in the forthcoming only the first harmonic and its phase are discussed.

The ranges of the variables investigated in the two-hundred runs made in this study are given in Table 1. Viscosities were measured using an Ostwald viscometer. Diffusion coefficients

Table 1. Ranges of Experimental Variables

Frequency, β	0.106-2.189 rad/s
Fluid head in variable head tank	17.1-37.5 cm
Amplitude of height fluctuation	3.25-4.9 cm
Fluctuation ratio	9.2-19.5% of average height
Electrode length/pipe diameter, L/D	0.0089-0.285
Average tube Reynolds no., Re	330-1,000
Schmidt no., Sc	3,100-4,050
Graetz no., Gz	4.74×10^6-2.83×10^8
Peclet no., Pe:	
for $L/D = 0.0089$	$Pe = 274$-399
0.0178	836-1,658
0.0445	5,100-13,900
0.0694	1.22×10^4-3.38×10^4
0.1406	5.09×10^4-1.12×10^5
0.285	2.19×10^5
Womersley no., ω_v	1.86-8.57
Dimensionless frequency, ω_d	117-493
Correlation variable, X_1	0.0779-8.54
Correlation variable, X_2	9.44-951

of the ferricyanide ion were measured by comparing experimental data for mass transfer in steady laminar flow with the Leveque solution. These steady data showed excellent agreement with the theoretical solution. It should be noted that the maximum amplitude ratio of the fluctuating head in the tank was 0.2. This is well below the value for which reverse flow could occur so for all the data the velocity was always positive. Further, it is seen that this is a small head perturbation so that a linearized analysis should be valid. It may also be seen that the Peclet number in some instances is considerably less than 5000 and therefore some of the data do not satisfy the criterion of Ling (1963), Equation (7a). Calculations from the weaker criterion, Equation (7b) showed that even in the worst case the boundary layer solution should have been valid over more than 92% of the electrode length. It will be seen later that in spite of this the data collected did not agree completely with the predictions of the boundary layer theory. The reason for this is not known at present.

RESULTS AND DISCUSSION

Complete tabulations of the data including the effects of individual parameters have been given by McFeeley (1972). Here we summarize the results and compare the data with the theoretical predictions.

Figures 3 and 4 show typical data for the amplitude ratio A_{cp} and the phase lag angle Φ_{cp} of the first harmonic plotted against the dimensionless frequency parameter ω_d for various length to diameter ratios of the mass transfer surface. (Since the system has no preferred length, the use of tube diameter to nondimensionalize the length is done only for convenience.) The tube Reynolds number ranged from 328 to 341 in these runs. Also plotted are theoretical predictions calculated from Equation (12) for the low frequency range and Equation (18) which is empirical (see below) for the high frequency range. In keeping with physical intuition, the amplitude decreases monotonically and the phase lag angle increase monotonically with increasing values of the dimensionless frequency ω_d. It may be seen that the data lie in the intermediate and high frequency range of the dimensionless frequency ω_d.

As seen in Table 1, the range of ω_v for all the data was between 1.86 and 8.57. From Figure 3 of Alabastro and Hellums (1969) (their ω is our ω_v) one may deduce that

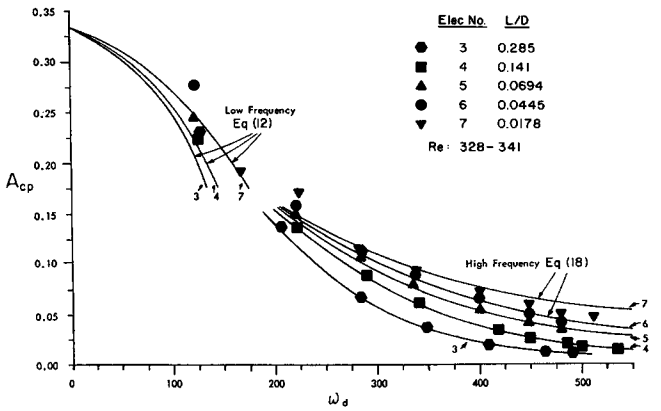

Fig. 3. Amplitude ratio A_{cp} for various frequencies and lengths of mass transfer element.

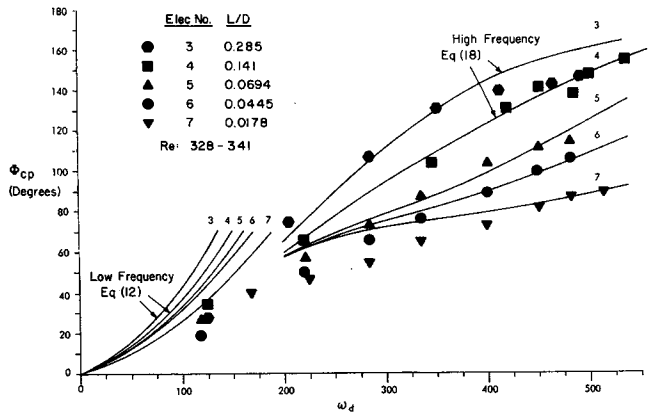

Fig. 4. Phase lag angle Φ_{cp} for various frequencies and lengths of mass transfer element.

this is very probably far outside the low frequency range. It is not possible to make a more definite statement because the figure cited is for the amplitude of the local mass transfer coefficient (point value) at a particular distance from the leading edge of the mass transfer surface. It was not found possible to take data for values of ω_d much less than 100, because as may be seen from the definition of ω_d, the only variable involved in ω_d that is readily changed is the frequency of oscillation β. The pipe radius R is fixed and the solution properties cannot be changed to any great extent so that ν and Sc are relatively fixed. In the equipment available, the motor speed, and hence β, could not be made low enough to achieve values of ω_d less than 100. (Future work is planned using a different gear ratio on the motor so that the low frequency range can be more completely investigated.) It is not surprising then that the low frequency solution does not agree very well with the data although in several cases the discrepancy is not appreciable.

It is also apparent that the phase angle data are more scattered than the amplitude ratio data. It is estimated that the measurement technique for the amplitude ratio, which involves a Fourier series fit of many data points for a single run is quite accurate. In contradistinction, the phase angle was calculated from only one measurement of the very short time interval (as low as 0.5 s) between the zero crossings of the oscillations of the displacement device and the electrode current. The phase angle data thus have larger relative error. From replicate runs for certain values of the parameters, the average deviation of A_{cp} was ± 1% whereas that for Φ_{cp} was ± 6.5% from the respective average values. For all the data it is estimated that the error in A_{cp} could be as high as ± 5% while the error in Φ_{cp} could be as high as ± 10 to 15%.

Figures 3 and 4 show very clearly the effect of the length of the transfer surface on the amplitude and phase. Again, in keeping with intuition, longer transfer surfaces give smaller values of the amplitude ratio and greater phase lags than shorter surfaces. This shows the capacitance effect of the diffusion boundary layer and is significant when using a diffusion-controlled electrode for wall shear measurements (for example Fortuna and Hanratty, 1972). It is also seen that the high frequency data fit [Equation (18)] provides excellent agreement with the data on A_{cp} and not as good agreement with the Φ_{cp} data.

Figures 5 and 6 are similar plots of A_{cp} and Φ_{cp} versus ω_d for a particular mass transfer length with the tube Reynolds number as a parameter. It is seen that in the range of variables investigated the effect of Reynolds number is slight. The data show in general that higher Reynolds numbers give greater amplitude ratios and smaller phase lags. This is physically reasonable.

McFeeley (1972) has presented further plots similar to Figures 3 to 6 for other data points. The trends are very similar. In general, data for higher frequencies (larger ω_d) show somewhat better agreement with the correlating equations than do data for lower ω_d. This is particularly true for the phase data, as may be seen in Figures 4 and 6. Possible explanations for this will be given below. The effect of individual variables such as electrode length, amplitude of pulsations, Schmidt number,

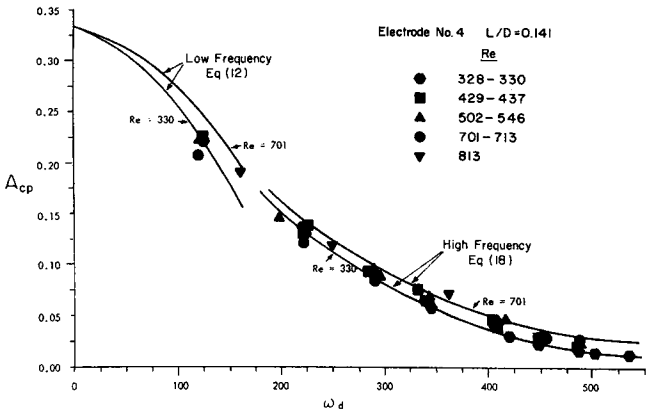

Fig. 5. Effect of Reynolds number on the amplitude ratio for fixed length of mass transfer element.

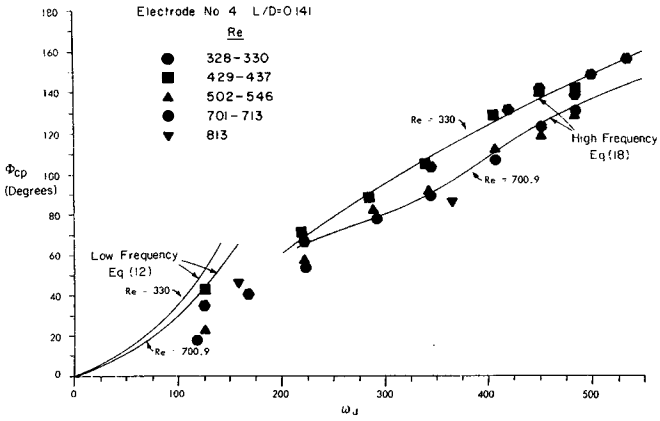

Fig. 6. Effect of Reynolds number on the phase lag angle for fixed length of mass transfer element.

Reynolds number, etc. have also been discussed in detail, and a complete tabulation of the data has been given by McFeeley (1972).

The theoretical analysis given above and the work of Pedley (1972) suggests that all the data may be correlated in terms of the variable $\omega_d^2\, Gz^{-2/3}$. Specifically, Equations (12) and (13) imply that the modulus and phase angle of the fluctuating mass transfer coefficient may be plotted in the form

$$A = \frac{A_{cp}}{M(\gamma/12)} = f(X_1) \tag{14}$$

and

$$\varphi = \Phi_{cp} - \Phi(\gamma/12) = g(X_1) \tag{15}$$

where

$$X_1 = \omega_d^2\, Gz^{-2/3} \tag{16}$$

Here $M(\gamma/12)$ represents the modulus and $\Phi(\gamma/12)$ the phase angle of the quantity $(\gamma/12)$. These can be calculated from Equation (3) since ω_v is known for each data point. Further, it should be noted that $M(\gamma/12)$ is related to the modulus and $\Phi(\gamma/12)$ is related to the phase angle of the fluctuating velocity [see Equation (2)]. Thus A is the ratio of the moduli of the fluctuating transfer coefficient and the fluctuating velocity and φ is the phase angle between the fluctuating transfer coefficient and the fluctuating velocity.

Although most of the data do not appear to be in the low frequency range, a test of the low frequency asymptote [Equation (12)] was made. Data points for the lower values of X_1 were chosen for this purpose. As may be seen in Table 1, X_1 for all the data fell in the range of 0.0779 and 8.54. All data points for $0 < X_1 < 0.4$ were used to test Equation (12). The choice of $X_1 = 0.4$ as the cutoff was arbitrary. Figures 7 and 8 are plots of A and φ respectively versus X_1 for these data points. It should be noted that all electrode lengths except the longest ($L/D = 0.285$) are represented on these figures. Further, the Reynolds number range is 330 to 1000, the Schmidt number range is 3100 to 4050 and the ω_d range is 117 to 360. Thus data for the higher values of L/D and ω_d are not plotted in Figures 7 and 8, but otherwise the complete ranges of fluctuation amplitude and Reynolds and Schmidt number are represented.

Figure 7 shows A plotted against X_1. It may be seen

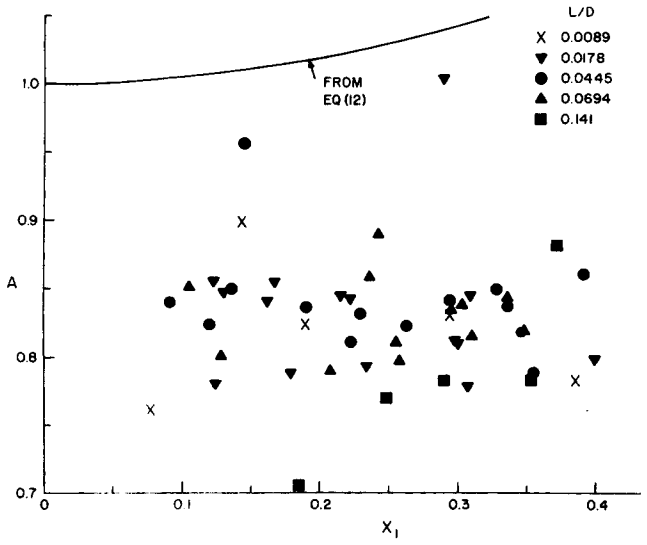

Fig. 7. The amplitude function A versus the variable X_1 (low frequencies).

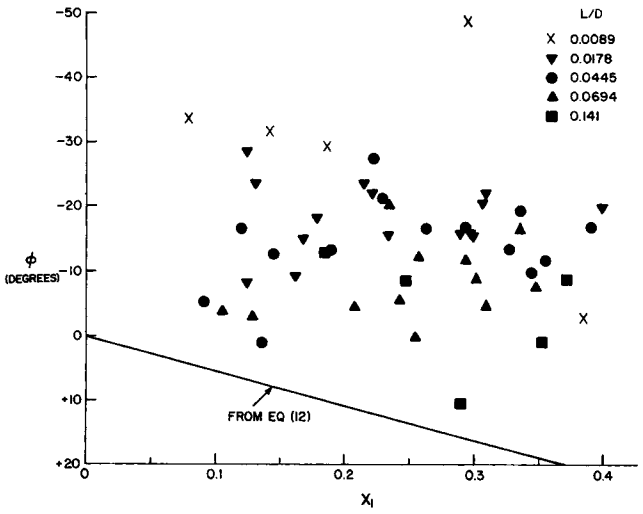

Fig. 8. The phase function φ versus the variable X_1 (low frequencies).

that the data scatter evenly (maximum deviation approximately ± 12%) around an ordinate value of about 0.825. There is no discernible increase or decrease with X_1. In this frequency range an asymptotic value of A appears to have been reached. It appears that the L/D ratio has no effect on the value of A, in accordance with Equation (14). The low frequency solution, Equation (12), for A is also shown and is seen to follow a trend similar to the low frequency solution given by Alabastro and Hellums (1969). It appears that the data values are not in the low frequency range as has been mentioned above. It is estimated that data need to be collected for values of X_1 of about 0.01 or less in order to test the low frequency asymptote.

Figure 8 is a plot of φ versus X_1. It is to be noted that all phase angles throughout this paper are plotted as lags. Thus φ represents the phase lag between the fluctuating mass transfer coefficient and the fluctuating velocity. Negative values of φ imply that the transfer coefficient is leading the velocity. Figure 8 shows that except for a few data points, the bulk of the data imply such a phase lead. From physical reasoning and from the theoretical model, it would appear that at low frequencies and small L/D ratios the phase lag between the transfer coefficient and the velocity will be very small. In the limit of zero frequency certainly there is no lag between transfer coefficient and velocity. Thus one would expect that the data of Figure 8 would show essentially zero or at most a small phase lag. It does not appear physically reasonable that the fluctuating coefficient should lead the fluctuating velocity. We believe that the reason for the negative values in Figure 8 is experimental error. The experimental data for phase are obtained by measuring the time elapsed between the zero crossings of the displacement device and the fluctuating current from the electrode. At low frequencies and small electrode lengths this time is very small ($\sim$ 0.5 s) and the measurement is subject to large error. Further, because of the slow changes, there is greater chance of drift in the amplifiers used to measure and control the circuit, causing further sources of error. Since φ is the difference between Φ_{cp} and $\Phi(\gamma/12)$, the latter being calculated, it is seen that negative values may result for small Φ_{cp} since the effect of measurement errors will be greatest in this case. For higher frequencies and larger (L/D) ratios, the relative errors are considerably less and the transfer coefficient is found to lag the velocity as expected. There is still considerable scatter in the data.

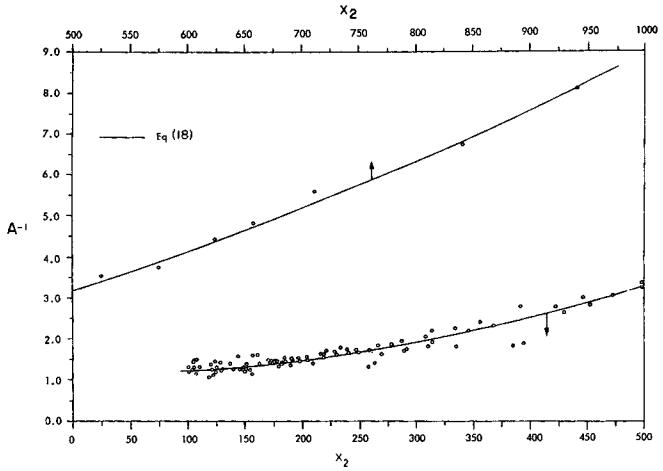

Fig. 9. The amplitude function A versus the correlation variable X_2 (high frequencies).

It seems clear that more accurate measurements of the phase are needed especially at lower frequencies in future work.

When the rest of the data were plotted in the form suggested by Equations (14) and (15) the behavior was different from that shown in Figures 7 and 8. A series of different curves resulted for different values of Reynolds number and ω_d. This effect was especially pronounced for larger values of X_1. This phenomenon is unexpected, in view of Equations (14) and (15), and it would seem that there are additional effects which are not predicted by the theory in this range of X_1. It is conceivable that the neglect of diffusion in the x-direction implicit in Equation (5) is responsible for this discrepancy, since as pointed out above, Ling's criterion was not satisfied for some of the data points. On the other hand, it is conceivable that the flow field was not sufficiently developed in the region of the test section. It is not possible at present to give the precise cause of this effect with any assurance. In the range of X_1 where this effect was pronounced, an attempt was made to obtain a new correlation variable so that the data fell on the same curve for all mass transfer lengths and Reynolds numbers. This variable, referred to as X_2, was found to be

$$X_2 = \omega_d^2 Gz^{-1/3}(L/D)^{1/3} \tag{17}$$

and has the same L/D dependence as X_1 but has a different dependence on the Reynolds and Schmidt numbers.

It is somewhat more convenient to plot A^{-1} versus X_2 as discussed below, and such a plot is shown in Figure 9. It may be seen that the data fall consistently along the same curve especially at large values of X_2. At lower values of X_2 the scatter is greater although more or less evenly distributed around the curve. Data values for $X_2 > 100$ only have been plotted, and the correlation shown is intended only for these higher values of X_2. At lower values of X_2 the scatter is similar to that for X_2 between 100 and 150 and, again, evenly distributed around the curve. From Figure 9 it is seen that the variable A decreases from a value of about 0.8 for $X_2 = 100$ to a value of about 0.12 for $X_2 = 950$. Since X_2 is proportional to ω_d^2 it is evident that the amplitude ratio is decreasing with frequency in agreement with physical reasoning.

The curve drawn in Figure 9 is an empirical curve fit of the data. The modulus of R_{cp} from Equation (13) is $\{1 + (aX_1)^2\}^{-1/2}$. This suggests a correlation for A^{-1} in the form of a power series in the new variable X_2. The curve shown in Figure 9 is calculated from such a power series correlation given by

$$A^{-1} = a_1 + a_2X_2 + a_3X_2^2 \tag{18}$$

The constants a_1, a_2, and a_3 were generated by a least squares fit to obtain

$$a_1 = 1.147$$
$$a_2 = 4.625 \times 10^{-4} \tag{19}$$
$$a_3 = 7.456 \times 10^{-5}$$

Since A^{-1} is given as a polynomial in X_2 it has been plotted in this way in Figure 9. It may be seen that the empirical curve, Equation (18), fits the data quite well at high values of X_2. The scatter is somewhat greater at lower values of X_2 (between 100 and 150). For still lower values of X_2 (less than 100) the data has not been plotted in Figure 9; the scatter in this range is very similar to that for X_2 between 100 and 150. It should be emphasized that Equation (18) is intended to fit data for large values of X_2. This may be seen in Figure 3 where the agreement is good for large ω_d (large X_2) and less so for smaller ω_d. It was found that Equation (18) with the above coefficients predicts all the data (including $X_2 < 100$) with an average error of 5.4%. This excellent agreement should not be misunderstood, since the even, but significant, scatter at low values of X_2 undoubtedly causes such a low average error value. However, the equation does represent in one parametric expression all of the data for all values of mass transfer length, pulsation amplitudes, Reynolds numbers, and frequencies employed in this study.

Figure 10 is a plot of φ against X_2 as suggested by Equation (15). As in the case of Figure 9, the correlation is intended for larger values of X_2 and data points for $X_2 > 100$ only have been plotted. In contrast with Figure 8 the data all show a phase lag between the fluctuating coefficient and the velocity. As noted above, for higher frequencies and (L/D) ratios (larger X_2) the errors causing the negative values in Figure 8 are less pronounced and positive values of φ (implying phase lag) are obtained. The measurement errors do produce a great deal more scatter in the phase data as seen in Figure 8 and in Figures 4 and 6. The curve drawn in Figure 10 is obtained from the form of Equation (18) and the empirically fitted constants of Equation (19). It is seen that the trend of the data is followed by Equation (18), but the data values deviate considerably from the curve although they are more or less evenly distributed around it. In keeping with physical intuition, the phase lag is seen to increase with increasing frequency.

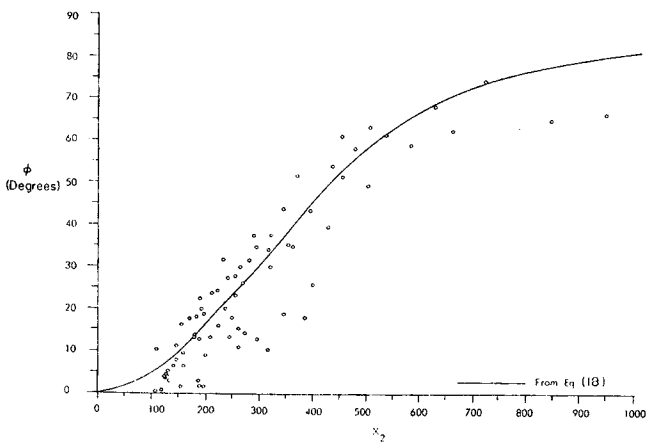

Fig. 10. The phase function φ versus the correlation variable X_2 (high frequencies).

It should be noted that perhaps another dimensionless variable could have been found that represents the data as well as the correlation variable X_2. What the present data seem to indicate is that the expected correlation with X_1 did not hold at higher values of X_1. It is certainly possible that measurement errors are responsible for this. One possible source of error is the exact nature of the flow field in the vicinity of the mass transfer surfaces. In future work some independent method of velocity measurement should be used to check the flow field near the electrode surfaces.

Time-averaged transfer coefficients have also been calculated for the data but are not reported in detail here. The change in the time-averaged transfer rate over the steady flow transfer rate at the same conditions was found to be quite small. This is consistent with the results of Alabastro and Hellums (1969) who report that it is the second harmonic of the fluctuating rate that contributes to this change. In the present study the second harmonic was small (generally an order of magnitude less than the first harmonic), and consequently little change in average transfer rate was observed. Work is continuing on this aspect of the problem and results will be reported.

ACKNOWLEDGMENT

This work is taken from the dissertation submitted by J. J. McFeeley to the Faculty of the Polytechnic Institute of Brooklyn in partial fulfillment of the requirements for the degree of Doctor of Philosophy (Chemical Engineering) 1972.

NOTATION

A = amplitude function, Equation (14)
A_{cp} = amplitude ratio of first harmonic of transfer coefficient
a_1, a_2, a_3 = constants
c = dimensionless concentration
c_0 = steady concentration
c_1 = first harmonic of concentration
D = pipe diameter
$\mathcal{D}$ = diffusion coefficient
Gz = Graetz number = $ReSc\ D/L$
K = mass transfer coefficient
$\langle K \rangle$ = spatially averaged mass transfer coefficient
$\langle K_s \rangle$ = steady part of $\langle K \rangle$
$\langle K_f \rangle$ = fluctuating part of $\langle K \rangle$
L = length of mass transfer surface (same as electrode length)
$M(\gamma/12)$ = modulus of $\gamma/12$
Pe = Peclet number based on mass transfer surface length = $4U_0L^2/R\mathcal{D}$
p = pressure
p_s = steady pressure
R = pipe radius
R_{cp} = ratio of fluctuating to steady transfer coefficient, Equation (12)
Re = pipe Reynolds number = DU_0/ν
Sc = Schmidt number = $\nu/\mathcal{D}$
t = time
U_0 = time-averaged mean velocity
u = velocity
X_1 = dimensionless correlation variable, Equation (16)
X_2 = dimensionless correlation variable, Equation (17)
x = coordinate in flow direction
y = coordinate normal to flow direction

Greek Letters

β = frequency
γ = function of ω_v, Equation (3)
λ_c = amplitude ratio, Equation (9)
λ_p = amplitude ratio of fluctuating pressure
ν = kinematic viscosity
Φ_{cp} = phase lag angle of first harmonic of transfer coefficient
$\Phi(\gamma/12)$ = phase of $\gamma/12$
φ = phase lag function, Equation (15)
ω_d = dimensionless frequency parameter = $\omega_v\ Sc^{1/2}$
ω_v = dimensionless frequency parameter (Womersley number) = $(\beta R^2/\nu)^{1/2}$

LITERATURE CITED

Alabastro, E. B. F., and J. D. Hellums, "A Theoretical Study on Diffusion in Pulsating Flow," *AIChE J.*, **15**, 2, 164 (1969).

Atabek, H. B., and C. C. Chang, "Oscillatory Flow near the Entry of a Circular Tube," *ZAMP*, **12**, 185 (1961).

Baird, M. H., G. J. Duncan, J. I. Smith, and J. Taylor, "Heat Transfer in Pulsed Turbulent Flow," *Chem. Eng. Sci.*, **21**, 197 (1966).

Eisenberg, M., C. W. Tobias and C. R. Wilke, "Ionic Mass Transfer and Concentration Polarization at Rotating Electrodes," *J. Electrochem. Soc.*, **101**, 306 (1954).

Fortuna, G., and T. J. Hanratty, "Frequency Response of the Boundary Layer on Wall Transfer Probes," *Intern. J. Heat Mass Transf.*, **14**, 1499 (1971).

Krusak, J. H., and J. M. Smith, "Mass Transfer in a Pulsed Column," *Chem. Eng. Sci.*, **18**, 591 (1963).

Lighthill, M. J., "The Response of Laminar Skin Friction and Heat Transfer to Fluctuation in the Stream Velocity," *Proc. Royal Soc. A*, **224**, 1 (1954).

Ling, S. C., "Heat Transfer from a Small Isothermal Spanwise Strip on an Insulated Boundary," *Trans. ASME, J. Heat Transfer, C85*, 230 (1963).

Martinelli, R. C., L. M. Boelter, E. B. Weinberg, and S. Yakahi, "Heat Transfer to a Fluid Flowing Periodically at Low Frequency in a Vertical Tube," *Trans. ASME*, **65**, 789 (1943).

McDonald, D. A., *Blood Flow in Arteries*, Edward Arnold, London (1960).

McFeeley, J. J., "The Response of a Diffusion-Controlled Electrode to Pulsed Laminar Flow," Ph.D. dissertation, Polytechnic Inst. Brooklyn, New York (1972).

McMichael, W. J., and J. D. Hellums, "Interphase Mass and Heat Transfer in Pulsatile Flow," *AIChE J.*, in press.

Mitchell, J. E., "An Investigation of Wall Turbulence Using a Diffusion Controlled Electrode," Ph.D. dissertation, Univ. Illinois, Urbana (1965).

Mueller, W. K., "Heat Transfer Characteristics of Periodically Pulsating Turbulent Pipe Flow," *Proc. Fifth Midwestern Conf. Fluid Mech.*, Ann Arbor, 146 (1957).

Ostrach, S., "Compressible Laminar Boundary Layer and Heat Transfer for Unsteady Motions of a Flat Plate," N.A.C.A., TN 3569 (1955).

Pedley, T. J., "On the Forced Heat Transfer from a Hot Film Embedded in the Wall in Two-dimensional Unsteady Flow," *J. Fluid Mech.*, **55**, pt. 2, 329 (1972).

Reiss, L. P., "Investigation of Turbulence near a Pipe Wall Using a Diffusion Controlled Electrolytic Reaction on a Circular Electrode," Ph.D. dissertation, Univ. Illinois, Urbana (1962).

Richardson, P. D., "Effect of Sound and Vibrations on Heat Transfer," *App. Mech. Rev.*, **20**, 201 (1967).

Romie, F. E., "Heat Transfer to Fluids Flowing with Velocity Pulsations in a Pipe," Ph.D. dissertation, Univ. of California, Los Angeles (1956).

Shirotsuka, T., "Mass Transfer through an Inner Tube Wall to Pulsating Flow," *Japan Chem. Eng.*, **21**, 287 (1957).

Sozin, Y. A., "Heat Transfer in a Pulsating Flow of an Incompressible Fluid," *Aviation Eng.*, **2**, 126 (1965).

Van Shaw, P., L. P. Reiss, and T. J. Hanratty, "Rates of Turbulent Transfer to a Pipe Wall in the Mass Transfer Entry Region," *AIChE J.*, **9**, 362 (1963).

West, F. B., and A. T. Taylor, "The Effect of Pulsation on Heat Transfer," *Chem. Eng. Progr.*, **48**, 1, 39 (1952).

Womersley, J. R., "Method for the Calculation of Velocity, Rate of Flow and Viscous Drag in Arteries When the Pressure Gradient Is Known," *J. Physiol.*, **127**, 553 (1955).

Manuscript received September 30, 1974; revision received and accepted November 21, 1974.